

# ACFNet: Attentional Class Feature Network for Semantic Segmentation

Fan Zhang<sup>1,2,3\*</sup> Yanqin Chen<sup>3</sup> Zhihang Li<sup>2</sup> Zhibin Hong<sup>3†</sup>  
Jingtuo Liu<sup>3</sup> Feifei Ma<sup>1,2†</sup> Junyu Han<sup>3</sup> Errui Ding<sup>3</sup>

<sup>1</sup> Laboratory of Parallel Software and Computational Science,  
Institute of Software, Chinese Academy of Sciences

<sup>2</sup> University of Chinese Academy of Sciences <sup>3</sup> Baidu Inc.

{zhangf, maff}@ios.ac.cn zhihang.li@nlpr.ia.ac.cn

{chenyanqin, hongzhibin, liujingtuo, hanjunyu, dingerrui}@baidu.com

## Abstract

Recent works have made great progress in semantic segmentation by exploiting richer context, most of which are designed from a spatial perspective. In contrast to previous works, we present the concept of class center which extracts the global context from a categorical perspective. This class-level context describes the overall representation of each class in an image. We further propose a novel module, named Attentional Class Feature (ACF) module, to calculate and adaptively combine different class centers according to each pixel. Based on the ACF module, we introduce a coarse-to-fine segmentation network, called Attentional Class Feature Network (ACFNet), which can be composed of an ACF module and any off-the-shell segmentation network (base network). In this paper, we use two types of base networks to evaluate the effectiveness of ACFNet. We achieve new state-of-the-art performance of 81.85% mIoU on Cityscapes dataset with only finely annotated data used for training.

## 1. Introduction

Semantic segmentation, which aims to assign per-pixel class label for a given image, is one of the fundamental tasks in computer vision. It has been widely used in various challenging fields like autonomous driving, scene understanding, human parsing, etc. Recent state-of-the-art semantic segmentation approaches are typically based on convolutional neural networks (CNNs), especially the Fully Convolution Network (FCN) frameworks [26].

One of the most effective approaches to improve the performance is exploiting richer context [46, 8, 12]. For ex-

\*This work is done when Fan Zhang is an intern at Baidu Inc.

†Corresponding Author

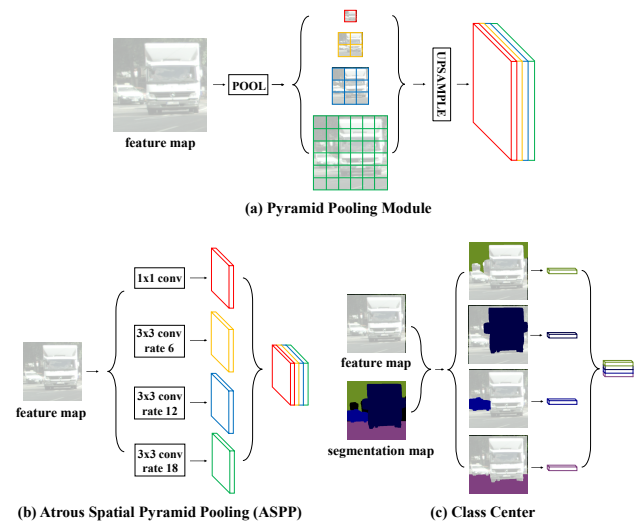


Figure 1. Different approaches to exploit context. The Pyramid Pooling Module (a) and the Atrous Spatial Pyramid Pooling (b) exploit context by employing different spatial sampling strategies. But the Class Center (c) captures the context via a categorical strategy, which uses all pixels of the same category to calculate a class-level feature.

ample, Chen *et al.* [8] proposed the atrous spatial pyramid pooling (ASPP) to aggregate spatial regularly sampled pixels at different dilated rates around a pixel as its context. In PSPNet [46], the pyramid pooling module divides the feature map into multiple regions with different sizes. The pooled representation of each region is then considered as the context within the same region. Moreover, the global average pooling (GAP) [23] is also widely used to obtain a global context [42, 46, 43, 8, 24]. Generally, these kinds of methods [9, 46, 12, 42, 43] focus on exploiting different spatial strategies to capture richer contextual informa-

tion. They do not distinguish pixels from different classes explicitly when calculating the context. Surrounding activated objects from different categories contribute the same to the context no matter what category the pixel comes from, which might be confusing for the pixel to determine which category it belongs to.

Different from the methods above, we argue that exploiting the class-level context, an ignored factor before, is also critical for semantic segmentation task. So in this work, we propose a new approach to exploit contextual information from a categorical perspective. We first present a so-called *class center* which describes the overall representation of each category in an image. Specifically, the class center of one class is the aggregation of all features of pixels belonging to this class. A comparison between class center and traditional context modules like ASPP [8] and PSP [46] is shown in Figure 1. ASPP and PSP try to exploit context by employing spatial strategies while the class center focuses on capturing the context from a categorical perspective which uses all pixels of the same category to calculate a class-level representation.

However, it is impractical to get the groundtruth label while testing. Hence, we propose a simple yet effective coarse-to-fine segmentation framework to approximate the class center. The class center for each class can be calculated by the coarse segmentation result and the high-level feature map of the backbone.

Moreover, inspired by the successful applications of attention mechanism in computer vision tasks, *e.g.* [47, 38, 16, 18], we put forward that different pixels need to adaptively pick up to class centers of different categories. For example, if there is no class of ‘road’ in an image, then pixels in this image do not need to focus on feature of ‘road’. Or if a pixel oscillates between class ‘person’ and class ‘rider’, it should pay more attention to how ‘person’ and ‘rider’ behave in the whole image rather than other categories. Therefore, an *attentional class feature* (ACF) module is proposed to use the attention mechanism to make pixels selectively be aware of different class centers of the whole scene. Different from previous works which design an independent module to learn the attention map, we directly use the coarse segmentation result as our attention map.

The overall structure of our proposed coarse-to-fine segmentation network, named *Attentional Class Feature Network*, is shown in Figure 2. More specifically, our proposed network consists of two parts. The first part is a complete semantic segmentation network, called *base network*, which generates coarse segmentation results and it can be any state-of-the-art semantic segmentation networks. The second part is our ACF module. The ACF module first uses the coarse segmentation result and the feature map in base network to calculate the class center for each category. After that, the attentional class feature is computed by coarse

segmentation result and class center. Finally, the attentional class feature and the original feature in base network are fused to generate the final segmentation.

We evaluate our *Attentional Class Feature Network* (ACFNet) on the popular scene parsing dataset Cityscapes [10] and it achieves new state-of-the-art performance of 81.85% mean IoU with only fine-annotated data for training.

Our contributions can be summarized as follows:

- We first present the concept of *class center*, which represents the class-level context, to help pixels be aware of the performance of different categories in the whole scene.
- The *Attentional Class Feature* (ACF) module is proposed to make different pixels adaptively focus on different class centers.
- We propose a coarse-to-fine segmentation structure, named *Attentional Class Feature Network* (ACFNet), to exploit class-level context to improve the semantic segmentation.
- ACFNet achieves new state-of-the-art performance of the mean IoU of 81.85% on the popular benchmark Cityscapes [10] dataset with only fine-annotated data for training.

## 2. Related Work

**Semantic Segmentation.** Benefiting from the advances of deep neural networks [20, 33, 34, 15, 17], semantic segmentation has achieved great success. The FCN [26] first replaces the fully connected layer in traditional classification network by convolutional layer to get a segmentation result. Segnet[2], RefineNet [22], Deeplabv3+ [9] and UNet [30] adopt encoder-decoder structure to carefully recover the reduced spatial information through step-by-step up-sample operation. Conditional random field (CRF) [6, 5, 7], Markov random field (MRF) [25] and Recurrent Neural Networks (RNNs) [4, 32] are also widely used to exploit the long-range dependencies. Dilated convolution [6, 44] is used to increase the feature resolution while reserving a large enough receptive field. In our work, we also use the same dilated strategy as in [46, 8] to preserve the resolution.

**Context.** Context plays a critical role in various vision tasks including semantic segmentation. There are bunches of works focusing on how to exploit more discriminative context to help the segmentation. Works like [42, 43] use global average pooling (GAP) to exploit the image level context. The atrous spatial pyramid pooling (ASPP) [8] is proposed to capture the nearby context based on different dilated rate. In PSPNet [46], the average pooling is employed over four different pyramid scales and pixels in one sub-region are treated as the context of pixels within the same sub-region. Some other works focus on how to fuse different context information [43, 42, 12, 28] more selec-

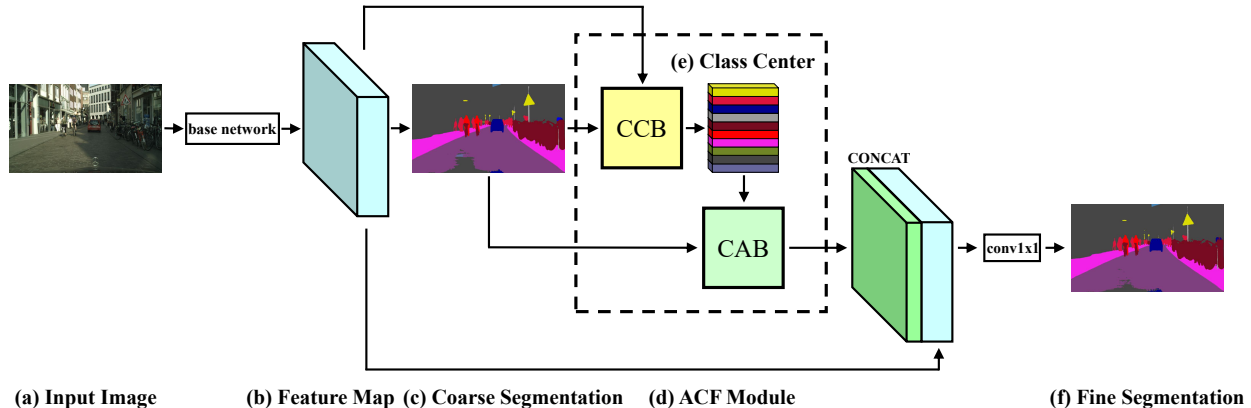


Figure 2. An Overview of the Attentional Class Feature Network. Given an input image (a), we first use a CNN (base network) to get the feature map of the higher layer (b) and the corresponding coarse segmentation result (c). Then an attentional class feature (ACF) module (d) is applied to calculate the class feature (e) of different categories and attentional class feature for each pixel according to their coarse segmentation result. Finally the attentional class feature and the feature map (b) are concatenated to get the final fine segmentation (f)

tively. In contrast to conventional context described above, in this paper, we harvest the contextual information from a categorical perspective.

More recently, a few works have also investigated the influence of the class-specific context. In EncNet [45], the channel-wise class-level features are enhanced or weakened according to the whole scene. Different from EncNet, we mainly focus on selectively utilizing the class-specific context from the pixel-level in our work.

**Attention.** Attention is widely used in various fields including natural language processing and computer vision. Vaswani *et al.* [35] proposed the transformer using self-attention for machine translation. Hu *et al.* [16] proposed object relation module to extend a learnable NMS operation. The non-local module [38] is proposed by Wang *et al.* to calculate the spatial-temporal dependencies. PSANet [47] also uses an attention map to aggregate long-range contextual information. Our work is inspired by the attention mechanism and we apply it to the calculation of attentional class feature. Instead of designing an independent module to learn the attention map as in previous works, we simply use the coarse segmentation result as the attention map.

**Coarse-to-fine Methods.** There are a lot of successful applications of using coarse-to-fine approaches, such as face detection [13], shape detection [1], face alignment [48] and optical flow [3]. Some existing segmentation networks [19, 49, 36, 21] also adopt coarse-to-fine strategy. Islam *et al.* [19] combined high resolution features and coarse segmentation result of low resolution features to get a finer segmentation result. In [49], rough locations of pancreas are obtained in the coarse stage and the fine stage is in charge of smoothing segmentation. In our work, we propose a coarse-to-fine structure and focus on improving the

final result through feature-level aggregation.

### 3. Methodology

In this section, we first introduce our proposed attentional class feature (ACF) module and elaborate how ACF module captures and adaptively combines the class centers. Then we introduce a coarse-to-fine segmentation structure which consists of our ACF module, named *Attentional Class Feature Network* (ACFNet).

#### 3.1. Attentional Class Feature Module

The overall structure of ACF module is shown in Figure.2 (d). It consists of two blocks, Class Center Block (CCB) and Class Attention Block (CAB) which are used to calculate class center and attentional class feature respectively. The attentional class feature (ACF) module is based on a coarse-to-fine segmentation structure. The input of the ACF module is the coarse segmentation result and the feature map in base network and the output is the attentional class feature.

##### 3.1.1 Class Center

The intuition of the concept of *class center* is to exploit richer global context from a categorical view. The class center of class  $i$  is defined as the average of features of all pixels belonging to class  $i$ . Ideally, given the feature map  $F \in \mathbb{R}^{C \times H \times W}$ , in which  $C$ ,  $H$  and  $W$  denote the number of channels, height and width of feature map respectively, the class center of class  $i$  can be formulated as follows,

$$F_{class}^i = \frac{\sum_{j=0}^{HW} \mathbb{1}[y_j = i] \cdot F_j}{\sum_{j=0}^{HW} \mathbb{1}[y_j = i]}, \quad (1)$$

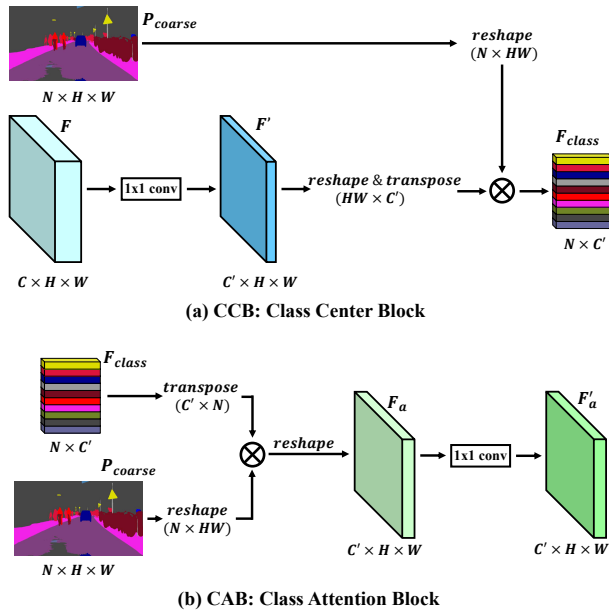


Figure 3. The details of Class Center Block (a) and Class Attention Block (b).

where  $y_j$  is the label of pixel  $j$  and  $\mathbb{1}[y_j = i]$  is the binary indicator that denotes whether the corresponding pixel comes from the  $i$ -th class.

Since the groundtruth label is not available during the test phase, we use the coarse segmentation result to evaluate how likely a pixel belongs to a specific class. For a certain class  $A$ , pixels with higher probability to  $A$  in coarse segmentation usually belong to  $A$ , and these pixels should contribute more when computing the class center of  $A$ . In this way, we can approximate a robust class center.

Given the coarse segmentation result  $P_{coarse} \in \mathbb{R}^{N \times H \times W}$  and the feature map  $F \in \mathbb{R}^{C \times H \times W}$ , where  $N$  is the number of categories, we propose a Class Center Block (CCB) to calculate the class center for each class. The structure of Class Center Block is shown in Figure 3 (a).

In order to calculate the class center with less computational cost, we first apply a channel reduction operation for feature map through a  $1 \times 1$  conv to reduce the channel number to  $C'$ . Then we reshape  $P_{coarse}$  to  $\mathbb{R}^{N \times HW}$  and the newly calculated feature map  $F'$  to  $\mathbb{R}^{C' \times HW}$ . After that we perform a matrix multiplication and normalization between the  $P_{coarse}$  and the transpose of  $F'$  to calculate the class centers  $F_{class} \in \mathbb{R}^{N \times C'}$ . Thus, Equation. 1 can be rewritten as follows:

$$F_{class}^i = \frac{\sum_{j=0}^{HW} P_{coarse}^{i,j} \cdot F'_j}{\sum_{j=0}^{HW} P_{coarse}^{i,j}}, \quad (2)$$

where  $P_{coarse}^{i,j}$  denotes the probability of pixel  $j$  belonging to class  $i$ . Both  $F'_j$  and  $F_{class}^i$  are in  $\mathbb{R}^{1 \times C'}$ .

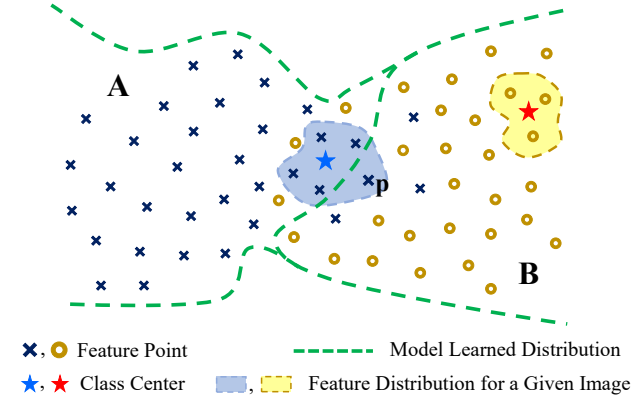


Figure 4. An illustration of the role of class center. For a given pixel  $p$  which belongs to class  $A$ , the model mislabels it to class  $B$  when only uses the feature of  $p$ . But if the model knows about the representation (class center) of  $A$  (light blue area) and  $B$  (light yellow area) in the image, it can find that  $p$  more likely comes from  $A$  rather than  $B$ . Thus, the wrong prediction could be corrected.

The benefits of class center are two-fold. Firstly, it allows the pixels to understand the overall presentation of each class from a global view. Since the class center is the combination of all pixels in an image, this gives a strong supervision information while training and can help the model learn more discriminative features for each class. Moreover, the class center can also help to check for the consistency between one pixel and each class center in the image to improve the performance. Therefore, the distribution of each class can be further refined. It is known that a model always learns the distribution of each category across the entire dataset, thus for a specific image, the distribution of a particular category often occupies a small portion of the distribution of that category over the entire dataset. So the class center of this portion is more representative and helpful for the pixel classification in this image. By introducing the class center, the model can correct many cases which are wrongly classified before. An example is shown in Figure 4, when only the feature of pixel  $p$  is used, the model mislabels it to class  $B$ . But the misclassification can be further fixed by considering the class centers at the same time.

### 3.1.2 Attentional Class Feature

Inspired by the attention mechanism, we present the attentional class feature. Different pixels need to selectively attend to different classes. For a pixel  $p$ , we use the coarse segmentation result as its attention map to calculate its attentional class feature. The reason why we use the coarse segmentation result is straightforward. If the coarse segmentation mislabels a pixel to a wrong class, it needs to pay more attention to that wrong class to check for the feature

consistency. Or if some classes do not even exist in the image, the pixel does not need to know about these classes. As in Figure 4, the pixel  $p$  only needs to be aware of the class centers of  $A$  and  $B$  rather than other class centers.

We propose a Class Attention Block (CAB) which is shown in Figure 3 (b) to calculate the attentional class feature. Given the class centers  $F_{class} \in \mathbb{R}^{N \times C'}$  and coarse segmentation result  $P_{coarse} \in \mathbb{R}^{N \times H \times W}$ , we first reshape  $P_{coarse}$  to  $\mathbb{R}^{N \times HW}$ . And then a matrix multiplication is applied to the transpose of  $F_{class}$  and  $P_{coarse}$  to calculate the attentional class feature  $F_a$  for each pixel. More specifically, the attentional class feature of pixel  $j$ , denoted as  $F_a^j$ , can be calculated as follows,

$$F_a^j = \sum_{i=0}^N P_{coarse}^{i,j} \cdot F_{class}^i, \quad (3)$$

where both  $F_a^j$  and  $F_{class}^i$  are in  $\mathbb{R}^{1 \times C'}$ .

After the attentional class feature is calculated, we apply a  $1 \times 1$  conv to refine the calculated feature.

### 3.2. Attentional Class Feature Network

Based on Attentional Class Feature (ACF) module, we propose the Attentional Class Feature Network for semantic segmentation as illustrated in Figure 2. ACFNet consists of two separate parts, base network and ACF module. The base network is a complete segmentation network. In our experiments, we use the ResNet [15] and ResNet with atrous spatial pyramid pooling (ASPP) [8] as our base networks respectively to verify the effectiveness of our ACF module. The ACF module leverages the segmentation result and feature map in base network to calculate the attentional class feature. Finally, we concatenate the attentional class feature and the feature map in base network together and refine it by a  $1 \times 1$  conv to get the final segmentation result.

**Loss Function.** For explicit feature refinement, we use the auxiliary supervision to improve the performance and make the network easier to optimize following PSPNet [46]. The class-balanced cross entropy loss is employed for auxiliary supervision, coarse segmentation and fine segmentation. Finally, we use three parameters  $\lambda_a$ ,  $\lambda_c$  and  $\lambda_f$  to balance the auxiliary loss  $l_a$ , the coarse segmentation loss  $l_c$  and the fine segmentation loss  $l_f$  as shown in Equation. 4

$$L = \lambda_a \cdot l_a + \lambda_c \cdot l_c + \lambda_f \cdot l_f. \quad (4)$$

## 4. Experiments

To evaluate the proposed module, we conduct several experiments on the Cityscapes [10] dataset. The Cityscapes dataset is collected for urban scene understanding, which contains 19 classes for scene parsing or semantic segmentation evaluation. It has 5,000 high resolution ( $2048 \times 1024$ )

images, of which 2,975 images for training, 500 images for validation and 1,525 for testing. In our experiments, we use the mean of class-wise Intersection over Union (mIoU) as the evaluation metric.

### 4.1. Network Architecture

We use two base networks to verify the effectiveness and generality of ACF module. One is ResNet-101 which is our baseline network and the other one is ResNet-101 with ASPP. The experiments on the latter network show that our module can also significantly improve the performance when combined with other state-of-the-art modules.

**Baseline Network.** As for baseline network, we use the ResNet-101 pre-trained on ImageNet [11]. Following PSPNet [46], the classification layer and last two pooling layers are removed and the dilation rate of the convolution layers after the removed pooling layers are set to 2 and 4 respectively. Thus, the output stride of the network is set to 8.

**Baseline Network with ASPP.** It is known that the atrous spatial pyramid pooling (ASPP) [8] has achieved great success in segmentation tasks. To verify the generalization ability of the ACF module, we also conduct several experiments based on the ResNet-101 (baseline network) followed by ASPP module. The ASPP consists of four parallel parts: a  $1 \times 1$  convolution branch and three  $3 \times 3$  convolution branches with dilation rate being 12, 24 and 36 respectively. In our re-implementation of ASPP module, we follow the original paper but change the output channel from 256 to 512 in all of four branches.

**Attentional Class Feature Module.** To reduce the computation and the memory usage, we first reduce the channel of input feature of ACF module to 512. The channel number of final output of the ACF module is also set to 512.

### 4.2. Implementation Details

For training, we use the stochastic gradient descent (SGD) optimizer [29] with the initial learning rate 0.01, weight decay 0.0005 and momentum 0.9 for Cityscapes dataset. Following the previous works [8, 46], we also employ the ‘poly’ learning rate policy, where the learning rate of current iteration is multiplied by the factor  $(1 - \frac{iter}{max.iter})^{0.9}$ . The loss weights  $\lambda_a$ ,  $\lambda_c$  and  $\lambda_f$  in Equation. 4 are set to 0.4, 0.6 and 0.7 respectively. All experiments are trained on  $4 \times$  Nvidia P40 GPUs for 40k iterations with batch size 8.

All BatchNorm layers in our network are replaced by InPlaceABN-Sync [31]. To avoid overfitting, we also employ the common data augmentation strategies, including random horizontal flipping, random scaling in the range of [0.5, 2.0] and random cropping of  $769 \times 769$  image patches following [46, 41].

### 4.3. Ablation Study

In this subsection, we conduct a series of experiments based on the baseline network to reveal the effect of each component in our proposed module.

#### 4.3.1 Attentional Class Feature module

We first use the atrous ResNet-101 as the baseline network and the final results are obtained by directly upsampling the output. For starters, we evaluate the performance of the baseline network, as shown in Table 1. It should be noted that all our experiments use the *auxiliary supervision*.

**Ablation for Class Center.** To verify the effect of class center, we first remove the Class Attention Block (CAB) in Figure 2 (d). The calculated class center  $F_{class}$  is reshaped and upsampled to  $\mathbb{R}^{NC \times H \times W}$ . Then the upsampled class center and the feature map in base network are concatenated to get the fine segmentation result. The experiment result is also shown in Table 1. This modification improves the performance to 76.42%(0.57% $\uparrow$ ) on coarse segmentation and 77.94% (2.09% $\uparrow$ ) on fine segmentation.

**Ablation for Attentional Class Feature.** We further evaluate the role of attentional class feature. Essentially, the calculation process described in Equation.3 is the weighted summation of class centers in which the weight is coarse segmentation probabilities of each pixel. So we call this approach of calculating the attentional class feature as **ACF(sum)**. Besides **ACF(sum)**, we also try another way, named **ACF(concat)**, to leverage the coarse segmentation probabilities and class centers to get another type of attentional class feature. For a given pixel  $j$ , **ACF(concat)** can be formulated as follows,

$$F_a^j = \text{CONCAT}_{i=0}^N \{ P_{coarse}^{i,j} \cdot F_{class}^i \}, \quad (5)$$

where  $F_a^j$  is in  $\mathbb{R}^{NC' \times 1}$  and it is the weighted concatenation of class centers in which the weight is coarse segmentation probabilities of each pixel. The experiment results are shown in Table 1. Compared with the experiment of class center, the **ACF(concat)** improves the performance of fine segmentation from 77.94% to 79.17% while the **ACF(sum)** achieves performance of 79.32%. When comparing with the baseline, the improvement is significant. In the following experiments, we use the **ACF(sum)** strategy as default.

#### 4.3.2 Feature Similarity

**Improvement Compared with Baseline.** In order to better understand how ACF module improves the final result, we visualize the cosine similarity map between a given pixel and other pixels in the feature map. As shown in Figure 5, we select two pixels from ‘terrain’ and ‘car’ respectively. The feature similarity maps of the baseline and ACFNet are shown in column (c) and (d) separately. For ACFNet, we

Method	mIoU(%)
ResNet-101 Baseline	75.85
ResNet-101 + class center	76.42(C) / 77.94(F)
ResNet-101 + ACF (concat)	76.66(C) / 79.17(F)
ResNet-101 + ACF (sum)	76.56(C) / 79.32(F)

Table 1. Detailed performance comparison of our proposed Attentional Class feature module on Cityscapes val. set based on the ResNet-101. **C**: result of coarse segmentation. **F**: result of fine segmentation. **ACF(concat)**: the attentional class feature is calculated by the weighted concatenation of class centers. **ACF(sum)**: the attentional class feature is calculated by the weighted summation of class centers.

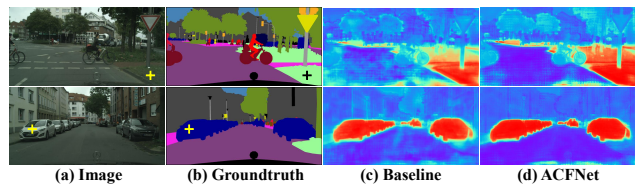


Figure 5. Feature similarity visualization of all pixels to a given pixel. Hotter color denotes more similar in feature level. The pixels we selected are marked as **cross sign** in (a) Image and (b) Groundtruth. Column (c) and (d) show the similarity maps of all other pixels to the selected pixel of baseline network and ACFNet.

use the feature map before fine segmentation to calculate the feature similarity. After adding the class-level context, ACFNet learns a more discriminative feature for each class. The intra-class features are more consistent and the inter-class features are more distinguishable.

#### Improvement Compared with Coarse Segmentation.

As discussed in section 3.1.1, the class-level context may also help a pixel check for the consistency with each class in the image and further refine the segmentation result. To verify this idea, we also visualize the feature similarity of the feature maps before coarse segmentation and fine segmentation given a specific pixel. As shown in Figure 6, the area which shows the improvement is marked by yellow square in both (e) coarse segmentation and (f) fine segmentation. From (b) and (e), we can see that the model does not learn a good enough distribution of class ‘building’ and thus mislabels a lot of pixels. Features of those mislabeled pixels are inconsistent with those correctly labeled pixels. But after adding the attentional class feature for those pixels, the refined feature shows the consistency between mislabeled pixels and correctly labeled pixels. Thus, the final result has a significant improvement.

#### 4.3.3 Result Visualization

We provide the qualitative comparisons between ACFNet and baseline network in Figure 7. We use the *yellow square*

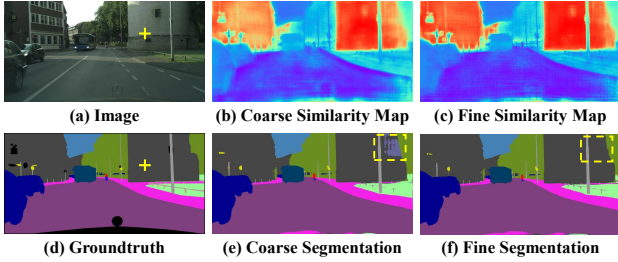


Figure 6. Feature similarity visualization of the feature maps before coarse segmentation and fine segmentation. The pixel selected to calculate the similarity with other pixels is marked by **cross sign** in (a) and (d). (b) and (c) show the similarity maps of feature maps before coarse segmentation and fine segmentation respectively. And the visual improvement part is marked by yellow square in (e) and (f).

to mark those challenging regions. The baseline easily mislabels such areas, but ACFNet is able to correct them. For example, the baseline model can not classify ‘truck’ or ‘car’ correctly in the first example and mislabels the ‘building’ and ‘wall’ in the fifth example. After adding the ACF module, such areas are greatly corrected.

#### 4.4. Experiments on Baseline Network with ASPP

To verify the generality of ACF module, we also combine it with ResNet-101 and ASPP. We first conduct the baseline (ResNet-101 with ASPP) experiment and the result is shown in Table 2. Our re-implemented version of ASPP achieves similar performance compared with the original paper [8] (78.42% vs. 77.82%).

**Performance with ACF Module.** We append the ACF module to the end of ASPP module and the experiment result is shown in Table 2. After adding the ACF module, the performance is improved by 1.7% (from 78.42% to 80.08%), which verifies that our ACF module can work together with other state-of-the-art modules to further boost the performance.

Moreover, we apply the online bootstrapping [39] and multi-scale (MS), left-right flipping (Flip) to improve the performance based on the ResNet-101+ ASPP + ACF. The results on Cityscapes val are shown in Table 2.

- **Online Bootstrapping:** Following the previous works [39], we adopt the online bootstrapping for hard training pixels. The hard training pixels are those whose probabilities on the correct classes are less than a certain threshold  $\theta$ . When training with online bootstrapping, we keep at least  $K$  pixels within each batch. In our experiments, we set  $\theta$  to 0.7 and  $K$  to 100,000. With online bootstrapping, the performance on Cityscapes val set can be improved by 0.91%.
- **MS/Flip:** As many of previous works [46, 43, 14, 41, 9], we also adopt the left-right flipping and multi-scale

Method	mIoU(%)
ResNet-101 + ASPP Baseline	78.42
ResNet-101 + ASPP + ACF	80.08
ResNet-101 + ASPP + ACF + OB	80.99
ResNet-101 + ASPP + ACF + MS/Flip	81.46

Table 2. Detailed performance comparison of our proposed Attentional Class feature module on Cityscapes val. set base on the ResNet-101 with ASPP. **ACF**: attentional class feature module. **OB**: using online bootstrapping while training. **MS/Flip**: using multi-scale and flipping while testing.

[0.75, 1.0, 1.25, 1.5, 1.75, 2.0] strategies while testing. From Table 2, we can see that **MS/Flip** improves the performance by 1.38% on val set.

#### 4.5. Comparing with the State-of-the-Art

We further compare ACFNet with the existing methods on the Cityscapes test set by submitting our result to the official evaluation server. Specifically, we train the ResNet-101 with ASPP and ACF with online bootstrapping strategy and use the multi-scale & flipping strategies while testing. The results and comparison are illustrated in Table 3. ACFNet, which uses only *train-fine* data, outperforms previous work PSANet [47] for about 2.2% and even better than most methods that also employ the validation set for training. While using both *train-fine* and *val-fine* data for training, ACFNet outperforms the previous methods [41, 47, 43, 42] for a large margin and achieves new state-of-the-art of 81.85% mIoU.

### 5. Conclusion

In this paper, we propose the concept of *class center* to represent the class-level context to improve the segmentation performance. We further propose a coarse-to-fine segmentation structure based on our attentional class feature module, called ACFNet, to calculate and selectively combine the class-level context according to the feature of each pixel. The ablation studies and visualization of intermediate results show the effectiveness of class-level context. ACFNet achieves new state-of-the-art on Cityscapes dataset with mIoU of 81.85%.

### 6. Acknowledgment

Feifei Ma is supported by the Youth Innovation Promotion Association, Chinese Academy of Sciences. Besides, our special thanks go to Yuchen Sun, Xueyu Song, Ru Zhang, Yuhui Yuan and the anonymous reviewers for the discussion and their helpful advice.

Methods	Mean IoU	road	sidewalk	building	wall	fence	pole	traffic light	traffic sign	vegetation	terrain	sky	person	rider	car	truck	bus	train	motorcycle	bicycle
PSPNet †[46]	78.4	-	-	-	-	-	-	-	-	-	-	-	-	-	-	-	-	-	-	-
PSANet †[47]	78.6	-	-	-	-	-	-	-	-	-	-	-	-	-	-	-	-	-	-	-
ACFNet (ours) †	<b>80.8</b>	98.7	87.1	93.7	60.8	62.0	69.7	77.7	80.4	94.0	73.6	95.7	87.6	73.6	96.1	65.6	87.3	83.0	70.5	78.0
DeepLab-v2 [7]	70.4	97.9	81.3	90.3	48.8	47.4	49.6	57.9	67.3	91.9	69.4	94.2	79.8	59.8	93.7	56.5	67.5	57.5	57.7	68.8
RefineNet ‡[22]	73.6	98.2	83.3	91.3	47.8	50.4	56.1	66.9	71.3	92.3	70.3	94.8	80.9	63.3	94.5	64.6	76.1	64.3	62.2	70
GCN ‡[27]	76.9	-	-	-	-	-	-	-	-	-	-	-	-	-	-	-	-	-	-	-
DUC ‡[37]	77.6	98.5	85.5	92.8	58.6	55.5	65	73.5	77.9	93.3	72	95.2	84.8	68.5	95.4	70.9	78.8	68.7	65.9	73.8
ResNet-38 [40]	78.4	98.5	85.7	93.1	55.5	59.1	67.1	74.8	78.7	93.7	72.6	95.5	86.6	69.2	95.7	64.5	78.8	74.1	69	76.7
BiSeNet ‡[42]	78.9	-	-	-	-	-	-	-	-	-	-	-	-	-	-	-	-	-	-	-
DFN ‡[43]	79.3	-	-	-	-	-	-	-	-	-	-	-	-	-	-	-	-	-	-	-
PSANet ‡[47]	80.1	-	-	-	-	-	-	-	-	-	-	-	-	-	-	-	-	-	-	-
DenseASPP ‡[41]	80.6	<b>98.7</b>	<b>87.1</b>	93.4	<b>60.7</b>	62.7	65.6	74.6	78.5	93.6	72.5	95.4	86.2	71.9	96.0	<b>78.0</b>	<b>90.3</b>	80.7	69.7	76.8
ACFNet (ours) ‡	<b>81.8</b>	<b>98.7</b>	<b>87.1</b>	<b>93.9</b>	60.2	<b>63.9</b>	<b>71.1</b>	<b>78.6</b>	<b>81.5</b>	<b>94.0</b>	<b>72.9</b>	<b>95.9</b>	<b>88.1</b>	<b>74.1</b>	<b>96.5</b>	76.6	89.3	<b>81.5</b>	<b>72.1</b>	<b>79.2</b>

†Training with only the *train-fine* dataset.

‡Training with both the *train-fine* and *val-fine* datasets.

Table 3. Per-class results on Cityscapes test set with the state-of-the-art models. ACFNet outperforms existing methods and achieves 81.8% in mIoU.

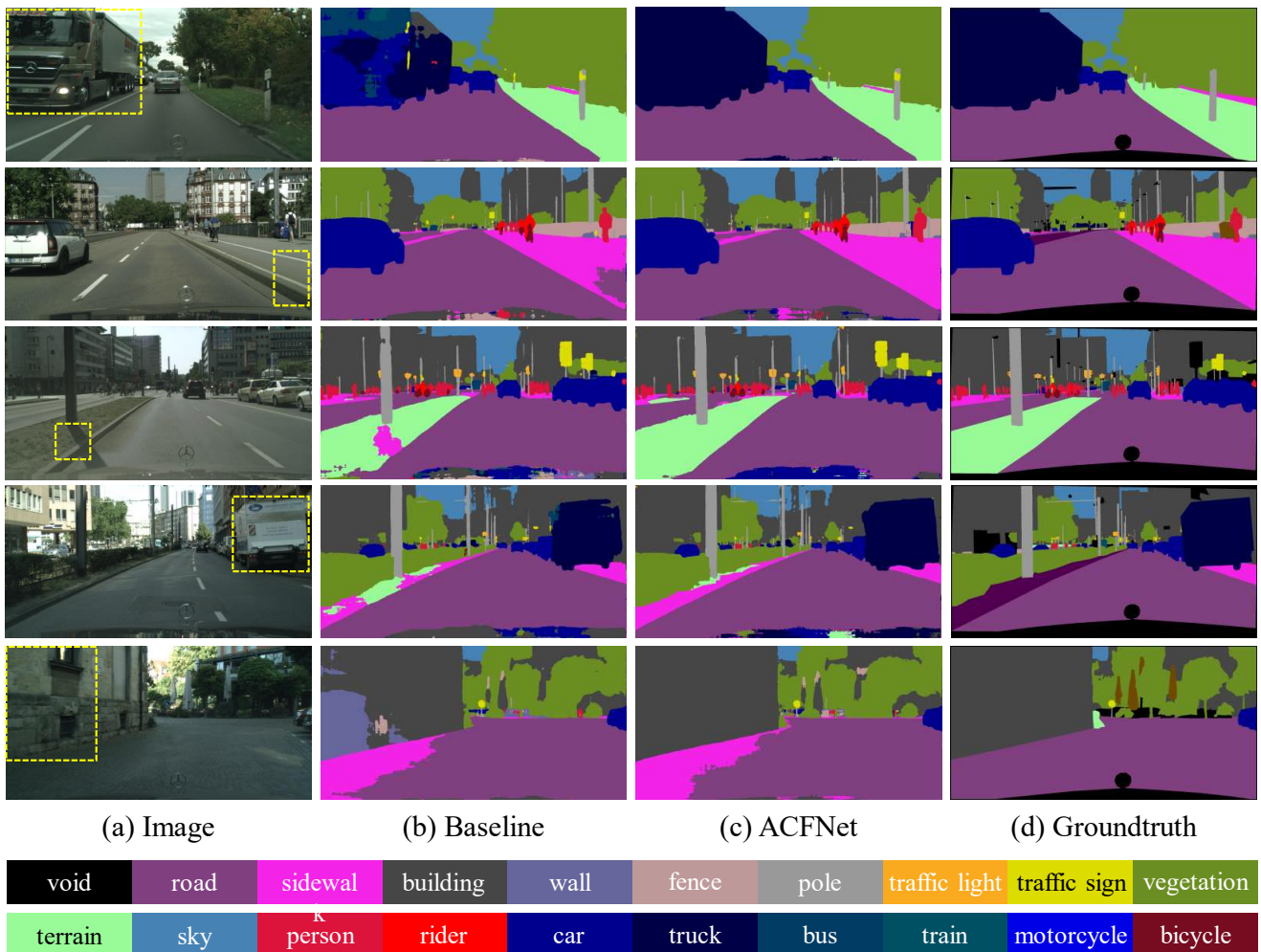


Figure 7. Visualization results of ACFNet based on ResNet-101 network on Cityscapes val set.

## References

- [1] Yali Amit, Donald Geman, and Xiaodong Fan. A coarse-to-fine strategy for multiclass shape detection. *IEEE Transactions on Pattern Analysis & Machine Intelligence*, (12):1606–1621, 2004.
- [2] Vijay Badrinarayanan, Alex Kendall, and Roberto Cipolla. Segnet: A deep convolutional encoder-decoder architecture for image segmentation. *IEEE transactions on pattern analysis and machine intelligence*, 39(12):2481–2495, 2017.
- [3] Thomas Brox, Andrés Bruhn, Nils Papenberg, and Joachim Weickert. High accuracy optical flow estimation based on a theory for warping. In *European conference on computer vision*, pages 25–36. Springer, 2004.
- [4] Wonmin Byeon, Thomas M Breuel, Federico Raue, and Marcus Liwicki. Scene labeling with lstm recurrent neural networks. In *Proceedings of the IEEE Conference on Computer Vision and Pattern Recognition*, pages 3547–3555, 2015.
- [5] Siddhartha Chandra, Nicolas Usunier, and Iasonas Kokkinos. Dense and low-rank gaussian crfs using deep embeddings. In *Proceedings of the IEEE International Conference on Computer Vision*, pages 5103–5112, 2017.
- [6] Liang-Chieh Chen, George Papandreou, Iasonas Kokkinos, Kevin Murphy, and Alan L Yuille. Semantic image segmentation with deep convolutional nets and fully connected crfs. *arXiv preprint arXiv:1412.7062*, 2014.
- [7] Liang-Chieh Chen, George Papandreou, Iasonas Kokkinos, Kevin Murphy, and Alan L Yuille. Deeplab: Semantic image segmentation with deep convolutional nets, atrous convolution, and fully connected crfs. *IEEE transactions on pattern analysis and machine intelligence*, 40(4):834–848, 2018.
- [8] Liang-Chieh Chen, George Papandreou, Florian Schroff, and Hartwig Adam. Rethinking atrous convolution for semantic image segmentation. *arXiv preprint arXiv:1706.05587*, 2017.
- [9] Liang-Chieh Chen, Yukun Zhu, George Papandreou, Florian Schroff, and Hartwig Adam. Encoder-decoder with atrous separable convolution for semantic image segmentation. *arXiv preprint arXiv:1802.02611*, 2018.
- [10] Marius Cordts, Mohamed Omran, Sebastian Ramos, Timo Rehfeld, Markus Enzweiler, Rodrigo Benenson, Uwe Franke, Stefan Roth, and Bernt Schiele. The cityscapes dataset for semantic urban scene understanding. In *Proc. of the IEEE Conference on Computer Vision and Pattern Recognition (CVPR)*, 2016.
- [11] Jia Deng, Wei Dong, Richard Socher, Li-Jia Li, Kai Li, and Li Fei-Fei. Imagenet: A large-scale hierarchical image database. 2009.
- [12] Henghui Ding, Xudong Jiang, Bing Shuai, Ai Qun Liu, and Gang Wang. Context contrasted feature and gated multi-scale aggregation for scene segmentation. In *Proceedings of the IEEE Conference on Computer Vision and Pattern Recognition*, pages 2393–2402, 2018.
- [13] Francois Fleuret and Donald Geman. Coarse-to-fine face detection. *International Journal of computer vision*, 41(1-2):85–107, 2001.
- [14] Jun Fu, Jing Liu, Haijie Tian, Zhiwei Fang, and Hanqing Lu. Dual attention network for scene segmentation. *arXiv preprint arXiv:1809.02983*, 2018.
- [15] Kaiming He, Xiangyu Zhang, Shaoqing Ren, and Jian Sun. Deep residual learning for image recognition. In *Proceedings of the IEEE conference on computer vision and pattern recognition*, pages 770–778, 2016.
- [16] Han Hu, Jiayuan Gu, Zheng Zhang, Jifeng Dai, and Yichen Wei. Relation networks for object detection. In *Proceedings of the IEEE Conference on Computer Vision and Pattern Recognition*, pages 3588–3597, 2018.
- [17] Gao Huang, Zhuang Liu, Laurens Van Der Maaten, and Kilian Q Weinberger. Densely connected convolutional networks. In *Proceedings of the IEEE conference on computer vision and pattern recognition*, pages 4700–4708, 2017.
- [18] Zilong Huang, Xinggang Wang, Lichao Huang, Chang Huang, Yunchao Wei, and Wenyu Liu. Ccnet: Criss-cross attention for semantic segmentation. *arXiv preprint arXiv:1811.11721*, 2018.
- [19] Md Amirul Islam, Shujon Naha, Mrigank Rochan, Neil Bruce, and Yang Wang. Label refinement network for coarse-to-fine semantic segmentation. *arXiv preprint arXiv:1703.00551*, 2017.
- [20] Alex Krizhevsky, Ilya Sutskever, and Geoffrey E Hinton. Imagenet classification with deep convolutional neural networks. In *Advances in neural information processing systems*, pages 1097–1105, 2012.
- [21] Weicheng Kuo, Anelia Angelova, Jitendra Malik, and Tsung-Yi Lin. Shapemask: Learning to segment novel objects by refining shape priors. *arXiv preprint arXiv:1904.03239*, 2019.
- [22] Guosheng Lin, Anton Milan, Chunhua Shen, and Ian Reid. Refinenet: Multi-path refinement networks for high-resolution semantic segmentation. In *Proceedings of the IEEE conference on computer vision and pattern recognition*, pages 1925–1934, 2017.
- [23] Min Lin, Qiang Chen, and Shuicheng Yan. Network in network. *arXiv preprint arXiv:1312.4400*, 2013.
- [24] Wei Liu, Andrew Rabinovich, and Alexander C Berg. Parsenet: Looking wider to see better. *arXiv preprint arXiv:1506.04579*, 2015.
- [25] Ziwei Liu, Xiao Xiao Li, Ping Luo, Chen-Change Loy, and Xiaoou Tang. Semantic image segmentation via deep parsing network. In *Proceedings of the IEEE international conference on computer vision*, pages 1377–1385, 2015.
- [26] Jonathan Long, Evan Shelhamer, and Trevor Darrell. Fully convolutional networks for semantic segmentation. In *Proceedings of the IEEE conference on computer vision and pattern recognition*, pages 3431–3440, 2015.
- [27] Chao Peng, Xiangyu Zhang, Gang Yu, Guiming Luo, and Jian Sun. Large kernel matters improve semantic segmentation by global convolutional network. In *Computer Vision and Pattern Recognition (CVPR), 2017 IEEE Conference on*, pages 1743–1751. IEEE, 2017.
- [28] Yao Qin, Konstantinos Kamnitsas, Siddharth Ancha, Jay Nanavati, Garrison Cottrell, Antonio Criminisi, and Aditya Nori. Autofocus layer for semantic segmentation. In *International Conference on Medical Image Computing and*

- Computer-Assisted Intervention*, pages 603–611. Springer, 2018.
- [29] Herbert Robbins and Sutton Monro. A stochastic approximation method. *The annals of mathematical statistics*, pages 400–407, 1951.
- [30] Olaf Ronneberger, Philipp Fischer, and Thomas Brox. U-net: Convolutional networks for biomedical image segmentation. In *International Conference on Medical image computing and computer-assisted intervention*, pages 234–241. Springer, 2015.
- [31] Samuel Rota Bulò, Lorenzo Porzi, and Peter Kotschieder. In-place activated batchnorm for memory-optimized training of dnns. In *Proceedings of the IEEE Conference on Computer Vision and Pattern Recognition*, pages 5639–5647, 2018.
- [32] Bing Shuai, Zhen Zuo, Bing Wang, and Gang Wang. Scene segmentation with dag-recurrent neural networks. *IEEE transactions on pattern analysis and machine intelligence*, 40(6):1480–1493, 2018.
- [33] Karen Simonyan and Andrew Zisserman. Very deep convolutional networks for large-scale image recognition. *arXiv preprint arXiv:1409.1556*, 2014.
- [34] Christian Szegedy, Wei Liu, Yangqing Jia, Pierre Sermanet, Scott Reed, Dragomir Anguelov, Dumitru Erhan, Vincent Vanhoucke, and Andrew Rabinovich. Going deeper with convolutions. In *Proceedings of the IEEE conference on computer vision and pattern recognition*, pages 1–9, 2015.
- [35] Ashish Vaswani, Noam Shazeer, Niki Parmar, Jakob Uszkoreit, Llion Jones, Aidan N Gomez, Łukasz Kaiser, and Illia Polosukhin. Attention is all you need. In *Advances in Neural Information Processing Systems*, pages 5998–6008, 2017.
- [36] Dan Wang, Xiujuan Chai, Hongming Zhang, Hong Chang, Wei Zeng, and Shiguang Shan. A novel coarse-to-fine hair segmentation method. In *Face and Gesture 2011*, pages 233–238. IEEE, 2011.
- [37] Panqu Wang, Pengfei Chen, Ye Yuan, Ding Liu, Zehua Huang, Xiaodi Hou, and Garrison Cottrell. Understanding convolution for semantic segmentation. In *2018 IEEE Winter Conference on Applications of Computer Vision (WACV)*, pages 1451–1460. IEEE, 2018.
- [38] Xiaolong Wang, Ross Girshick, Abhinav Gupta, and Kaiming He. Non-local neural networks. In *Proceedings of the IEEE Conference on Computer Vision and Pattern Recognition*, pages 7794–7803, 2018.
- [39] Zifeng Wu, Chunhua Shen, and Anton van den Hengel. High-performance semantic segmentation using very deep fully convolutional networks. *arXiv preprint arXiv:1604.04339*, 2016.
- [40] Zifeng Wu, Chunhua Shen, and Anton Van Den Hengel. Wider or deeper: Revisiting the resnet model for visual recognition. *Pattern Recognition*, 90:119–133, 2019.
- [41] Maoke Yang, Kun Yu, Chi Zhang, Zhiwei Li, and Kuiyuan Yang. Denscaspp for semantic segmentation in street scenes. In *Proceedings of the IEEE Conference on Computer Vision and Pattern Recognition*, pages 3684–3692, 2018.
- [42] Changqian Yu, Jingbo Wang, Chao Peng, Changxin Gao, Gang Yu, and Nong Sang. Bisenet: Bilateral segmentation network for real-time semantic segmentation. In *Proceedings of the European Conference on Computer Vision (ECCV)*, pages 325–341, 2018.
- [43] Changqian Yu, Jingbo Wang, Chao Peng, Changxin Gao, Gang Yu, and Nong Sang. Learning a discriminative feature network for semantic segmentation. In *Proceedings of the IEEE Conference on Computer Vision and Pattern Recognition*, pages 1857–1866, 2018.
- [44] Fisher Yu and Vladlen Koltun. Multi-scale context aggregation by dilated convolutions. *arXiv preprint arXiv:1511.07122*, 2015.
- [45] Hang Zhang, Kristin Dana, Jianping Shi, Zhongyue Zhang, Xiaoang Wang, Amrith Tyagi, and Amit Agrawal. Context encoding for semantic segmentation. In *The IEEE Conference on Computer Vision and Pattern Recognition (CVPR)*, 2018.
- [46] Hengshuang Zhao, Jianping Shi, Xiaojuan Qi, Xiaogang Wang, and Jiaya Jia. Pyramid scene parsing network. In *IEEE Conf. on Computer Vision and Pattern Recognition (CVPR)*, pages 2881–2890, 2017.
- [47] Hengshuang Zhao, Yi Zhang, Shu Liu, Jianping Shi, Chen Change Loy, Dahua Lin, and Jiaya Jia. Psanet: Point-wise spatial attention network for scene parsing. In *Proceedings of the European Conference on Computer Vision (ECCV)*, pages 267–283, 2018.
- [48] Shizhan Zhu, Cheng Li, Chen Change Loy, and Xiaoou Tang. Face alignment by coarse-to-fine shape searching. In *Proceedings of the IEEE conference on computer vision and pattern recognition*, pages 4998–5006, 2015.
- [49] Zhuotun Zhu, Yingda Xia, Wei Shen, Elliot K Fishman, and Alan L Yuille. A 3d coarse-to-fine framework for automatic pancreas segmentation. *arXiv preprint arXiv:1712.00201*, 2017.